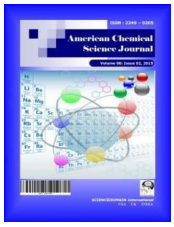

*American Chemical Science Journal*
*10(3): 1-9, 2016, Article no.ACSJ.21692*
*ISSN: 2249-0205*

**SCIENCEDOMAIN** *international*
www.sciencedomain.org

# Removal of High-Concentration Fe(III) by Oxidized Multiwall Carbon Nanotubes in a Fixed Bed Column

**Yongchao Li[1*], Xiaoxian Hu[1], Bozhi Ren[1] and Zhenghua Wang[1]**

*[1]School of Civil Engineering, Hunan University of Science and Technology, China.*

***Authors' contributions***

*This work was carried out in collaboration between all authors. Author YL designed the study and wrote the manuscript. Author XH carried out the experimental work and author BR analysed the experimental data. Author ZW revised the manuscript. All authors read and approved the final manuscript.*

***Article Information***

DOI: 10.9734/ACSJ/2016/21692
Editor(s):
(1) Jaya Narayan Sahu, Chemical Engineering Department, University of Malaya, Malaysia.
Reviewers:
(1) Oupa Ntwampe, University of North West, South Africa.
(2) Imran Ali, Central University, India.
(3) Honória de Fátima Gorgulho, Universidade Federal de São João del Rei, Brazil.
Complete Peer review History: http://sciencedomain.org/review-history/11938

***Original Research Article***

***Received 29th August 2015***
***Accepted 3rd October 2015***
***Published 23rd October 2015***

## ABSTRACT

The use of modified multiwall carbon nanotubes (MWCNTs) for high concentration of ferric iron removal from acid mine drainage was studied. Fourier transform infrared spectrum demonstrated that hydroxyl and carbonyl functional groups were introduced to the surface of MWCNTs after oxidation with nitric acid. The adsorption behavior of modified MWCNTs was then investigated in removing 50-200 mg/L Fe(III) through batch and continuous flow fixed bed experiments. Batch experiment results demonstrated that the Fe(III) adsorption capability of MWCNTs after oxidation had increased by 32%. Adsorption equilibrium was achieved during the first 90 min. Langmuir model can be successfully employed for the equilibrium of isotherms with $R^2$=0.9878 and $q_{max}$=89.05 mg/g. In addition, the effect of column bed depths and the influent Fe(III) concentrations were studied through the continuous fixed-bed adsorption studies. Results indicated that Fe(III) uptake favoured particularly higher bed depth and lower influent concentration. The bed uptake capacity of Fe(III) was found to be in a range of 30.30-41.51 mg/g, which was much lower than in batch experiment.

*Keywords: Adsorption; ferric ions; fixed-bed column system; oxidized multiwall carbon nanotubes.*

---

**Corresponding author: E-mail: nkliyongchao@163.com;*

## 1. INTRODUCTION

Along the development of industry and agriculture, heavy metal pollution of terrestrial and aquatic ecosystems seems to escalate more seriously [1]. Most of all, mining of ore deposits that contain large amounts of sulfide minerals and heavy metals pollutes the environment tremendously [2]. The oxidation of pyritic mining waste is a self-perpetuating corrosive process which continuously generates acid mine drainage (AMD). The AMD is an acidic wastewater and rich in sulfates, dissolved iron, cadmium, lead, copper, and arsenic [3]. Moreover, the ferric iron ions is predominant in the AMD waters, and the concentration can be as high as several hundred milligrams per liter [4,5]. The presence of total iron of more than 0.3 mg/L may cause anorexia, oliguria and diphasic shock. And the large quantity iron can give a metallic taste and odor to water [6]. It is therefore imperative that serious attention should be paid on the removal of high concentration of ferric iron from the AMD waters.

Heavy metals in the AMD waters are usually treated by adding alkaline materials such as lime, fly ash and alkaline industrial wastes and form precipitate as hydroxides [7-9]. Major disadvantages of this method are the need for continuous addition of the materials, low reaction rates, and the production of huge amounts of wastes [10]. Recently, adsorption onto solid adsorbent is reported to be the potential alternative technique to remove the pollutants from the wastewater [11-15]. Carbon nanotubes were first discovered by Iijima in 1991 [16]. The novel and interesting graphitic carbon materials has been proven to have an ability of excellent adsorption capacity in the removal heavy metal ions and organic pollutants [17-19] from aqueous solutions, as a result of high specific surface area and strong interactions between carbon atoms and hydrogen molecules. In addition, the adsorption capacity of carbon nanotubes can be improved by surface modifications, such as oxidization [20,21] and other chemical or physical modifications [22,23]. Rao et al. [24] have investigated the adsorption efficiency of carbon nanotubes towards divalent heavy metal ions, such as $Ni^{2+}$, $Pb^{2+}$, $Cd^{2+}$, $Cu^{2+}$ and $Zn^{2+}$, in which their adsorption capacity was significantly improved by their oxidation with acid solutions. However, the study on the adsorption of high concentration of Fe(III) onto MWCNTs is still very limited in the literature.

The efficiency of an adsorption process is usually controlled by the overall adsorption rate, which depends on transport processes outside and inside the adsorbent particles as well as the kinetics of binding. Over the years, the batch experiment has become the most commonly used configuration in wastewater treatment. However, the adsorption efficiency in a fixed-bed adsorption column is a function of the liquid flow pattern (axial and radial mixing) through the porous bed of particles and the liquid residence time. Furthermore, in practical wastewater treatment process, continuous fixed-bed adsorption experiments are most likely preferable, and the experimental data obtained from the studies are important for industrial applications [25].

The objective in this present study is to evaluate the performance of oxidized MWCNTs in the removal of Fe(III) from aqueous solution through batch and continuous fixed-bed system. The specific objectives are to (1) prepare and characterize oxidized MWCNTs, (2) test the Fe(III) removal by oxidized MWCNTs in batch experiment and calculate the parameters of adsorption isotherms, (3) study the effect of bed depth and initial Fe(III) concentration on breakthrough curve in the fixed-bed system.

## 2. EXPERIMENTAL WORK

### 2.1 Materials and Methods

The pristine MWCNTs were purchased from Beijing boyu gaoke new material technology Co., Ltd, China. All the chemicals and reagents used were analytical grade. A stock solution of Fe(III) (1000 mg/L) was prepared by dissolving ferric chloride in deionized water. The solution was further diluted to the required concentrations and the pH of the solutions was adjusted by using 0.1 mol/L hydrochloric acid or sodium hydroxide solutions.

### 2.2 Oxidation of MWCNTs

The pristine MWCNTs were prepared using chemical vapor deposition method. The outer diameter was about 10-20 nm, inner diameter was 5-10 nm, and the length was 10-30 μm. Its special surface area was more than 200 $m^2/g$, and the purity was higher than 95%. The pristine MWCNTs were oxidized by using nitric acid to remove the hemispherical caps and the particles of catalyst at the tips of nanotubes. 3 g of pristine

MWCNTs were immersed in 50 mL concentrated nitric acid for 24 h, and then washed with deionized water until the solution pH reached 6.5, dried in the oven at 105℃ for 4 h, and used in the following experiments.

### 2.3 Characterization of MWCNTs

For characterization of the functional groups on the surface of MWCNTs, Fourier transform infrared (FTIR, 560E.S.P, Nicolet, USA) spectra of samples were measured by the standard KBr disk method.

### 2.4 Batch Experiments

Adsorption experiments were carried out in serum bottles at a temperature of 25℃. The pH of Fe (III) solution was adjusted to 3.5 using 1.0 mol/L HCl solution prior to the experiment. A certain amount of pristine and oxidized MWCNTs were added to 50 mL of Fe(III) solution respectively. All reactors were agitated on a shaker at a rate of 180 revolutions per minute during the experiment. Samples were withdrawn at appropriate time intervals, filtered through a 0.22 μm membrane. The samples were analyzed for total iron concentrations using 1, 10-phenanthroline spectrophotometry [26]. Duplicate tests were conducted in all the experiments.

#### 2.4.1 Isotherm models

In order to gain a better understanding of the mechanism and to quantify the sorption data, Langmuir [27] and Freundlich [28] isotherm models are used to simulate the sorption of Fe(III) onto the oxidized MWCNTs. The equations of Langmuir isotherm model is expressed by:

$$\frac{1}{q_e} = \frac{1}{K_L C_e q_m} + \frac{1}{q_m} \quad (1)$$

where "$q_e$" is Fe(III) amount adsorbed on oxidized MWCNTs surface at equilibrium (mg/g); "$C_e$" is equilibrium concentration or final concentration of Fe(III) ions in the aqueous solution (mg/L); ''$q_m$'' is the maximum sorption capacity (mg/g); "$K_L$" is the Langmuir sorption constant (L/mg) which is related to the energy of adsorption.

The equations of Freundlich isotherm model can be expressed by:

$$\ln q_e = \ln K_f + \frac{1}{n} \ln C_e \quad (2)$$

where "$K_f$'' and ''n'' are the Freundlich constants which are indicators of adsorption capacity and adsorption intensity. The slopes and intercepts of the linear Langmuir and Freundlich plots are used to calculate the Langmuir and Freundlich constants.

### 2.5 Continuous Fixed-bed Adsorption Study

The breakthrough curve of Fe(III) was determined through continuous fixed-bed adsorption studies. The studies were conducted in a column made of glass tube with an internal diameter of 2.0 and 50 cm in length. The tube was packed with quartz sand. A layer of glass wool with 1 cm thickness was placed at the bottom of the column to prevent the adsorbent from leaching out, as well as on the top of the column to provide a uniform flow of the solution through the column. After the oxidized MWCNTs were packed in the column at a known quantity (1, 2 and 3 g) to yield the desired bed depth of 10, 20 and 30 cm, each column was flushed with 150 mg/L of Fe(III) solution. At the bed depth of 20 cm (equivalent to 2 g MWCNTs), known concentration of Fe(III) solutions (150, 200 and 300 mg/L) was pumped in a upward flow mode at a flow rate of 3 mL/min, respectively. The effluent samples at the outlet of the column were collected and analyzed for total iron concentrations at regular time intervals, and the column was operated until the concentration of Fe(III) exceeded 99.5% of its initial concentration. The experiments were carried out at room temperature, and the solution pH was adjusted to 3.5.

## 3. RESULTS AND DISCUSSION

### 3.1 Characterization of Pristine and Oxidized MWCNTs

Fig. 1 shows the FTIR spectra of pristine and oxidized MWCNTs. As shown in Fig. 1, the spectrum of pristine MWCNTs displayed three main bands at 1380, 1620, and 3440 $cm^{-1}$. However, these peaks became sharper after oxidation with nitric acid especially at 1380 $cm^{-1}$. The peak at 3440 $cm^{-1}$ can be assigned to the stretching vibration of O–H band. The signature of C=O functional groups was evident at 1620

$cm^{-1}$. The peak at 1380 $cm^{-1}$ was associated with C–H deformation vibration from aliphatic $–CH_3$ and $–CH_2$. New bands at 830 $cm^{-1}$ appeared in oxidized MWCNTs due to the bending of –C=O in carboxylic acid [29]. These peaks implied that oxidation by nitric acid was an effective process to introduce a lot of oxygen containing functional groups on the surfaces of MWCNTs.

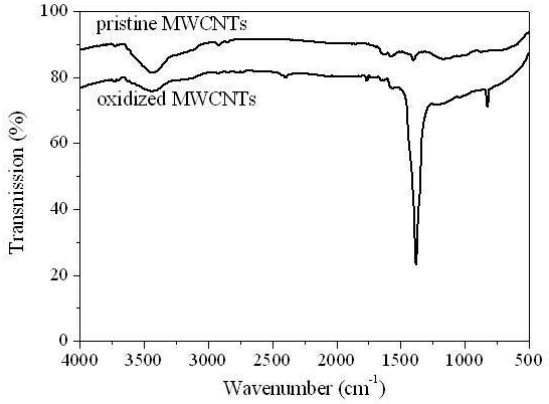


**Fig. 1. FTIR spectra of pristine and oxidized MWCNTs**

## 3.2 Comparison of Fe(III) Adsorption on Pristine and Oxidized MWCNTs

The objective of adsorption experimental exercise was to investigate the adsorption capacity of oxidized MWCNTs for Fe(III) ion. The adsorption of Fe(III) on the pristine and oxidized MWCNTs as a function of contact time (Fig. 2) showed that the adsorption ratio of Fe(III) onto MWCNTs after oxidation was improved significantly. The adsorption ratio of pristine Fe(III) was 43% while the adsorption capacity increased to 75% for the oxidized MWCNTs at the same reaction condition. This significant adsorption improvement was due to the increasing oxygen-containing functional groups and the total number of acid site on MWCNTs, which provided a large number of chemical adsorption sites [17]. It is apparent that the specific surface area, pore volume and average pore diameter of MWCNTs increased after oxidation was also a factor, which is in agreement with Perez-Aguilar's study [30].

The adsorption percentage of Fe(III) on MWCNTs increased rapid in the first 1 h, and then slowed down as equilibrium was approached. The contact time to reach equilibrium was about 90 min. The high initial adsorption rate may be attributed to the existence of large number of adsorption sites on the surface of MWCNTs. As the sites filled up gradually, the adsorption became slow and the mechanism of kinetics became more dependent on the rate at which the adsorptive was transported from the bulk phase to the actual adsorption sites. The adsorption reached equilibrium very quickly, which also indicated that the chemical adsorption or surface complexation rather than physical adsorption was the main sorption mechanism of Fe(III) on MWCNTs.

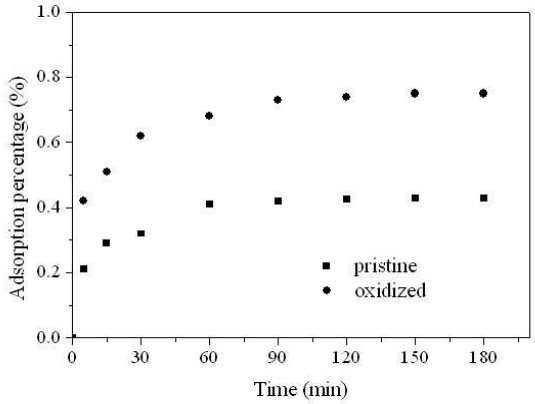


**Fig. 2. Comparison of Fe(III) adsorption ratio on pristine and oxidized MWCNTs. Initial MWCNTs dose: 1 g/L, initial Fe(III) concentration: 50 mg/L**

## 3.3 Adsorption Isotherms

Fig. 3 shows the removal of 50 mg/L Fe(III) ions using different dosages of oxidized MWCNTs. The removal percentage increased sharply while the adsorption capacity decreased with a rise in MWCNT mass. The removal ratio reached 96 % at the MWCNTs dosage of 1.6 g/L as a result of increasing number of the adsorption site in the MWCNTs adsorbent.

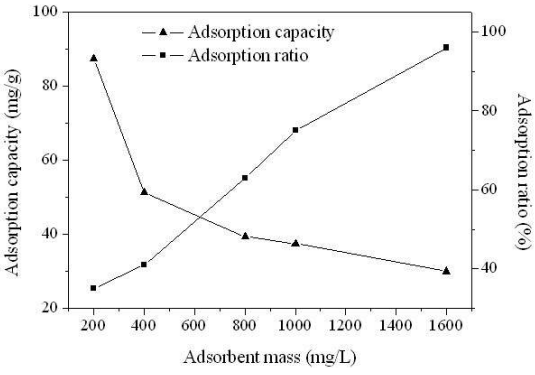


**Fig. 3. Fe(III) adsorption to MWCNTs with increasing adsorbent dose. Initial Fe(III) concentration: 50 mg/L, adsorbent dose: 0.2, 0.4, 0.8, 1.0, 1.6 g/L**

The effect of initial Fe(III) concentrations (50, 80, 120, 150 and 200 mg/L) on Fe(III) adsorption percentage was studied. As shown in Fig. 4, the Fe(III) equilibrium concentration and adsorption capacity increased by increasing initial Fe(III) concentration under the specific experimental conditions. However, the adsorption percentage of Fe(III) decreased with increasing initial concentration when the MWCNTs mass was same. For example, the removal percentage was 75 % at initial Fe(III) concentration of 50 mg/L, while it was 37 % at initial Fe(III) concentration of 200 mg/L. This phenomenon can be explained by the fact that, at the same MWCNT dosage, there was constant number of functional groups available on MWCNT surface. Therefore, the increase of Fe(III) concentration caused a decrease in the adsorption percentage of Fe(III).

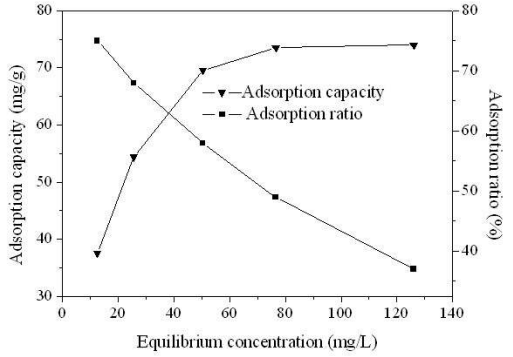


**Fig. 4. Fe(III) adsorption to MWCNTs with increasing equilibrium aqueous Fe(III) concentration. Initial Fe(III) concentration: 50, 80, 120, 150, 200 mg/L, MWCNTs dose: 1 g/L**

The equilibrium adsorption data of Fe(III) for oxidized MWCNTs was approximated by Langmuir and Freundlich isotherm models. The Freundlich model assumed that different sites with several adsorption energies were involved, whereas the Langmuir model predicts that there was no interaction between the adsorbate molecules and the adsorption was localized in a monolayer [31]. The linear plot of $1/q_e$ versus $1/C_e$ is shown in Fig. 5. According to the slope and intercepts (Fig. 5), the maximum adsorption capacity of Fe(III) and Langmuir adsorption constant of oxidized MWCNTs are calculated in Table 1 and the linear plot of $\ln q_e$ versus $\ln C_e$ is shown in Fig. 6. The calculated Freundlich parameters, $K_F$ and 1/n, from the slope and intercepts (Fig. 6) were also tabulated in Table 1.

As shown in Table 1, the adsorption data of Fe(III) for oxidized MWCNTs were fitted to the Langmuir equation. The correlation coefficients of the linear regressions ($R^2$) were found to be 0.9878. Freundlich model showed no correlation with the experimental data. That it indicated that the Langmuir model fitted the adsorption equilibrium data better than the Freundlich model. At the same time, the Fe(III) adsorption to oxidized MWCNTs was based on chemical adsorption and that is supported by the FTIR analysis.

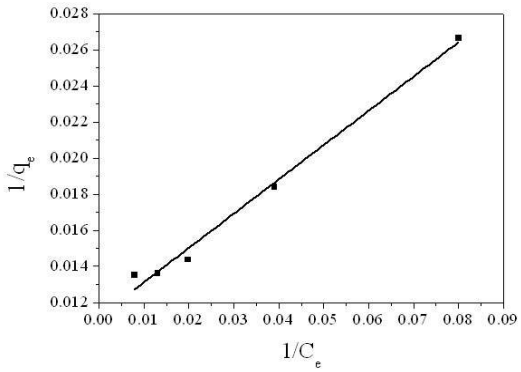


**Fig. 5. Langmuir isotherm of Fe(III) adsorption to MWCNTs**

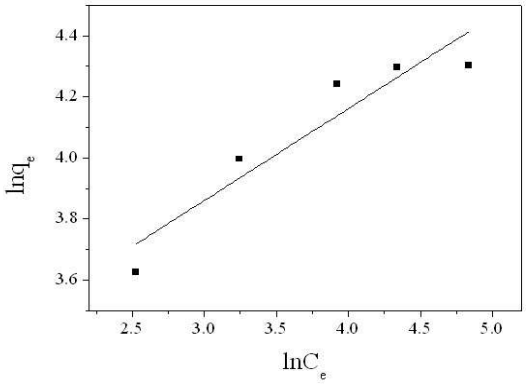


**Fig. 6. Freundlich isotherm of Fe(III) adsorption to MWCNTs**

## 3.4 Column Experiments

The breakthrough characteristics from column experimental results revealed information about adsorption behavior and adsorbent capacity. The effluent Fe(III) concentration was a function of time and can be presented in the form of a breakthrough curve. Fig. 7 shows the breakthrough curves obtained for 150 mg/L Fe(III) adsorption onto different column bed depths of 10 cm (1 g), 20 cm (2 g), and 30 cm (3 g) at a constant flow rate of 3 mL/min. Ct/C0 is the ratio of the outlet and inlet Fe(III) concentration as a function of time.

**Table 1. Langmuir and Freundlich isotherm parameters of Fe(III) adsorption to MWCNTs**

| Langmuir | | | Freundlich | | |
|---|---|---|---|---|---|
| $Q_{max}$ mg/g | $K_L$ L/mg | $R^2$ | 1/n | $K_F$ | $R^2$ |
| 89.05 | 0.059 | 0.9878 | 0.30 | 19.21 | 0.8545 |

Fig. 7 showed that the breakthrough curves exhibited a characteristic S shape with varying degrees of steepness under three different operating conditions. The position of the breakpoint was different. The first few layers of fresh oxidized MWCNTs were able to adsorb the Fe(III) rapidly and effectively during the initial stages of operation. However, after 175 min of adsorption the removal rate of Fe(III) dropped to 0 in the 10 cm long fixed-bed column. As the bed depth increased to 30 cm, the exhaustion time increased to 350 min. The increase of MWCNTs mass at higher bed depth led to an increase in the volume of treated effluent. In general, Fe(III) ions adsorption in a fixed-bed column system was highly associated with the quantity of oxidized MWCNTs [32, 33]. In essence, the mass transfer zone in a column moved from the entrance of the bed and proceeded to the top of the column. Therefore, an increase in bed depth, broadened the mass transfer zone and enlarged the distance to reach the exit resulting in an extended breakthrough time.

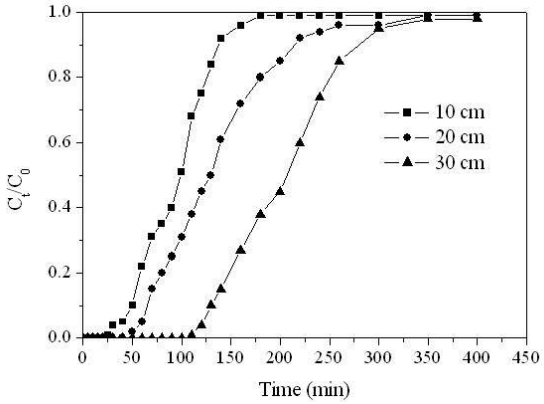


**Fig. 7. Breakthrough curves for adsorption of Fe(III) onto oxidized MWCNTs at different bed depths**

In addition, Fe(III) uptake capacity in column experiment was in a range of 30.30-41.51 mg/g, which was much lower than in batch experiment. It was because the MWCNTs dispersion was not effective, which then reduced the effective area. In addition, the flow rate of water in the column experiment was much lower, thus causing a reduction in mass transfer.

Fig. 8 shows the effect of Fe(III) influent concentrations on the breakthrough curves by varying the concentrations to 150, 200 and 300 mg/L and bed depth of 20 cm. In this study, high-range concentration of metal solution was employed to obtain a breakthrough curve as acid main drainage was found within this range [5]. As illustrated in Fig. 8, the MWCNTs beds reached faster saturation with the increasing influent Fe(III) concentration. The breakthrough curves were steeper as the influent concentration increased, indicating that higher influent concentrations led to higher driving force for mass transfer; hence, the adsorbent achieved saturation faster, which also resulted in a decreasing exhaust time [34]. However, the adsorption capacity for Fe(III) increased with higher influent metal concentration. The highest bed capacities of oxidized MWCNTs for adsorption of Fe(III) were 35.3 mg/g, at influent metal concentration of 200 mg/L.

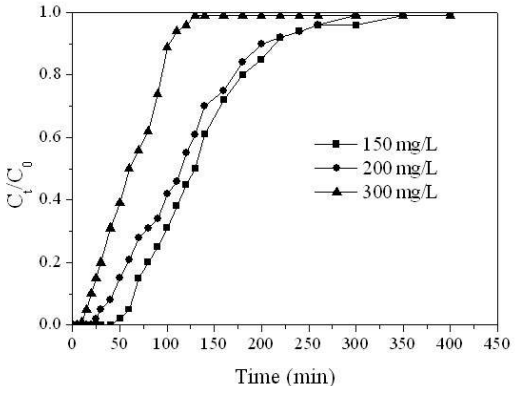


**Fig. 8. Breakthrough curve for adsorption of Fe(III) onto the oxidized MWCNTs at different influent concentrations**

## 3.5 Comparison of Adsorption Capacity for the Removal of Fe(III) Using Various Adsorbents

The adsorption capacities of different adsorbents used for the removal of Fe(III) ions are listed in Table 2. It was found that the oxidized MWCNTs undoubtedly contained high adsorption capacity, indicating it is potential to be utilized as a natural adsorbent for heavy metal removal from wastewater effluent.

**Table 2. Comparison of adsorption capacities of Fe(III) with other adsorbents**

| Type of adsorbent | pH | Temperature ℃ | $q_{max}$ mg/g | Reference |
|---|---|---|---|---|
| Natural feldspar | 1.15 | 30℃ | 25 | [35] |
| Chitosan | 3.0 | 25℃ | 90.09 | [36] |
| Acid activated clays | 3.0 | 30℃ | 30.00 | [37] |
| Eggshells | 6.0 | 20℃ | 5.99 | [38] |
| Modified resin | 2.5 | 20℃ | 179 | [39] |
| Oxidized MWCNTs | 3.5 | 25℃ | 89.05 | This study |

## 4. CONCLUSIONS

The modification of MWCNTs by nitric acid was verified by FTIR and it indicated that different functional groups such as carboxylic and hydroxyl were formed. In batch studies, the adsorption of Fe(III) was dependent on initial Fe(III) concentration, adsorbent dose. The Langmuir model fitted the adsorption equilibrium data better than the Freundlich model. Fe(III) removal in a fixed bed confirmed a faster approach to saturation when the mass of the MWCNTs was low and initial concentrations of Fe(III) were high. This study demonstrated that the oxidized MWCNTs could be utilized as an effective adsorbent for the removal of high concentration Fe(III) from aqueous solution in batch experiment or a fixed-bed column system.

## ACKNOWLEDGEMENTS

This work was supported by the National Natural Science Foundation of China (No. 51504094), the Research Foundation of Education Department of Hunan Province, China (No. 13C310) and the Scientific Research Fund of Hunan Provincial Education Department, China (Grant No. 10K027).

## COMPETING INTERESTS

Authors have declared that no competing interests exist.

## REFERENCES

1. Ali I, Aboul-Enein HY. Instrumental methods in metal ions speciation: Chromatography, capillary electrophoresis and electrochemistry. Taylor & Francis Ltd., New York, USA; 2006.
2. Banks D, Younger PL, Arnesen RT, Iversen ER, Banks SB, Mine-water chemistry: The good, the bad and the ugly. Environmental geology. 1997;32:157-174.
3. Lottermoser B. Mine wastes characterization, Treatment and environmental impacts, Springer: Berlin; 2003.
4. Wingenfelder U, Hansen C, Furrer G, Schulin R. Removal of heavy metals from mine waters by natural zeolites. Environmental Science & Technology. 2005;39(12):4606-4613.
5. Zheng YJ, Peng YL, Le HC, Li CH. Separation and recovery of Zn, Fe and Mn in acid mine drainage. Journal of Central South University (Science and Technology). 2011;42(7):1858-1864.
6. Michalakos GD, Nieva JM, Vayenas DV, Lyberatos G. Removal of iron from potable water using a trickling filter. Water Research. 1997;31(5):991-996.
7. Madzivire G, Petrik LF, Gitari WM, Ojumu TV, Balfour G. Application of coal fly ash to circumneutral mine waters for the removal of sulphates as gypsum and ettringite. Minerals Engineering. 2010;23:252-257.
8. Alakangas L, Andersson E, Mueller S. Neutralization/prevention of acid rock drainage using mixtures of alkaline by-products and sulfidic mine wastes. Environmental Science and Pollution Research. 2013;20(11):7907-7916.
9. Khorasanipour M, Moore F, Naseh R. Lime treatment of mine drainage at the Sarcheshmeh porphyry copper mine, Iran. Mine Water and the Environment, 2011; 30(3):216-230.
10. Ziemkiewicz PF, Skousen JG, Simmons J. Long-term performance of passive acid mine drainage treatment systems. Mine Water and the Environment. 2003;22: 118-129.
11. Ali I, Gupta VK. Advances in water treatment by adsorption technology. Nature Protocols. 2007;1(6):2661–2667.
12. Ali I. The quest for active carbon adsorbent substitutes: Inexpensive adsorbents for toxic metal ions removal from wastewater, Separation & Purification Reviews. 2010; 39(3-4):95-171.

13. Ali I, Asim M, Khan TA. New generation adsorbents for water treatment. Chemical Reviews. 2012;112:5073-5091.
14. Ali I, Asim M, Khan TA. Low cost adsorbents for removal of organic pollutants from wastewater. Journal of Environmental Management. 2012;113: 170-183.
15. Imran A. Water treatment by adsorption columns: Evaluation at ground level. Separation & Purification Reviews. 2014; 43:175-2015.
16. Iijima S. Helical microtubules of graphitic carbon. Nature. 1991;354:56-58.
17. Yu JG, Zhao XH, Yu LY, Jiao FP, Jiang JH, Chen XQ. Removal, recovery and enrichment of metals from aqueous solutions using carbon nanotubes. Journal of Radioanalytical and Nuclear Chemistry. 2014;299(3):1155-1163.
18. Vadahanambi S, Lee SH, Kim WJ, and Oh Il-Kwon. Arsenic removal from contaminated water using three-dimensional graphene-carbon nanotube-iron oxide nanostructures. Environmental Science & Technology. 2013;47(18): 10510-10517.
19. Vecitis CD, Gao GD, Liu H. Electrochemical carbon nanotube filter for adsorption, desorption, and oxidation of aqueous dyes and anions. The Journal of Chemical Physics. 2011;115(9):3621-3629.
20. Ye YL, Tang YQ, Niu ZL, Su L, Guo ZJ, Wu WS. Experiment and modeling of the interaction of copper(II) and salicylic acid with oxidized multi-walled carbon nanotubes. Colloids and Surfaces A: Physicochemical and Engineering Aspects. 2014;451:16-24.
21. Wang JP, Ma XX, Fang GZ, Pan MF, Ye XK, Wang S. Preparation of iminodiacetic acid functionalized multiwalled carbon nanotubes and its application as sorbent for separation and preconcentration of heavy metal ions. Journal of Hazardous Materials. 2011;186:1985-1992.
22. Alothman ZA, Habila M, Yilmaz E, Soylak M. Solid phase extraction of Cd(II), Pb(II), Zn(II) and Ni(II) from food samples using multiwalled carbon nanotubes impregnated with 4-(2-thiazolylazo) resorcinol. Microchim Acta. 2012;177:397-403.
23. Yoo DH, Rue GH, Seo JY, Hwang YH, Chan MHW, and Kim HK. Study of argon adsorbed on open-ended carbon nanotube bundles. Journal of Physical Chemistry B. 2002;106(35):9000-9003.
24. Rao GP, Lu C, Su F. Sorption of divalent metal ions from aqueous solution by carbon nanotubes: A review. Separation and Purification Technology. 2007;58: 224-231.
25. Baral SS, Das N, Ramulu TS, Sahoo SK, Das SN, Chaudhury G.R. Removal of Cr (VI) by thermally activated weed Salvinia cucullata in a fixed-bed column. Journal of Hazardous Materials. 2009;161:1427-1435.
26. APHA-AWWA-WEF. Standard methods for examination of water and wastewater (20th ed)". American Public Health Association, Washington DC; 1998.
27. Langmuir I. The constitution and fundamental properties of solids and liquids. Journal of the American Chemical Society. 1916;38:2221–2295.
28. Freundlich HMF. Uber die adsorption in losungen. Z Phys Chem (Leizig). 1906;57A: 385–470.
29. Sun WL, Zhou K. Adsorption of 17β-estradiol by multi-walled carbon nanotubes in natural waters with or without aquatic colloids. Chemical Engineering Journal. 2014;258:185-193.
30. Perez-Aguilar NV, Muñoz-Sandoval E, Diaz-Flores PE, Rangel-Mendez JR. Adsorption of cadmium and lead onto oxidized nitrogen-doped multiwall carbon nanotubes in aqueous solution: Equilibrium and kinetics. Journal of Nanoparticle Research. 2010;12:467-480.
31. Chen C, Li X, Zhao D, Tan X, Wang X. Adsorption kinetic, thermodynamic and desorption studies of Th(IV) on oxidized multi-wall carbon nanotubes. Colloids and Surfaces A. 2007;302:449-454.
32. Ahmad AA, Hameed BH. Fixed-bed adsorption of reactive azo dye onto granular activated carbon prepared from waste. Journal of Hazardous Materials. 2010;175:298-303.
33. Qaiser S, Saleemi AR. Umar M. Biosorption of lead from aqueous solution by *Ficus religiosa* leaves: Batch and column study. Journal of Hazardous Materials. 2009;166:998-1005.
34. Baral SS, Das N, Ramulu TS, Sahoo SK, Das SN, Chaudhury GR. Removal of Cr (VI) by thermally activated weed Salvinia cucullata in a fixed-bed column. Journal of Hazardous Materials. 2009;161:1427-1435.
35. Al-Anber M. Adsorption of ferric ions onto natural feldspar: Kinetic modeling and

adsorption isotherm. International Journal of Environmental Science & Technology. 2013;12(1):139-150.
36. Wan WS, Ghani SA, Kamari A. Adsorption behavior of Fe(II) and Fe(III) ions in aqueous solution on chitosan and cross-linked chitosan beads. Bioresource Technology. 2005;96:443-450.
37. Bhattacharyya KG, Gupta SS. Adsorption of Fe(III) from water by natural and acid activated clays: Studies on equilibrium isotherm, kinetics and thermodynamics of interactions. Adsorption. 2006;12(3): 185-204.
38. Yeddou N, Bensmaili A. Equilibrium and kinetic of iron adsorption by eggshells in a batch system: Effect of temperature. Desalination. 2007;206:127-134.
39. Khalil MMH, Al-Wakeel KZ, Rehim SSAE, Monem HAE. Efficient removal of ferric ions from aqueous medium by amine modified chitosan resins. Journal of Environmental Chemical Engineering. 2013;15:66-573.



*Peer-review history:*
*The peer review history for this paper can be accessed here:*
*http://sciencedomain.org/review-history/11938*